

1 **Supplemental Information**

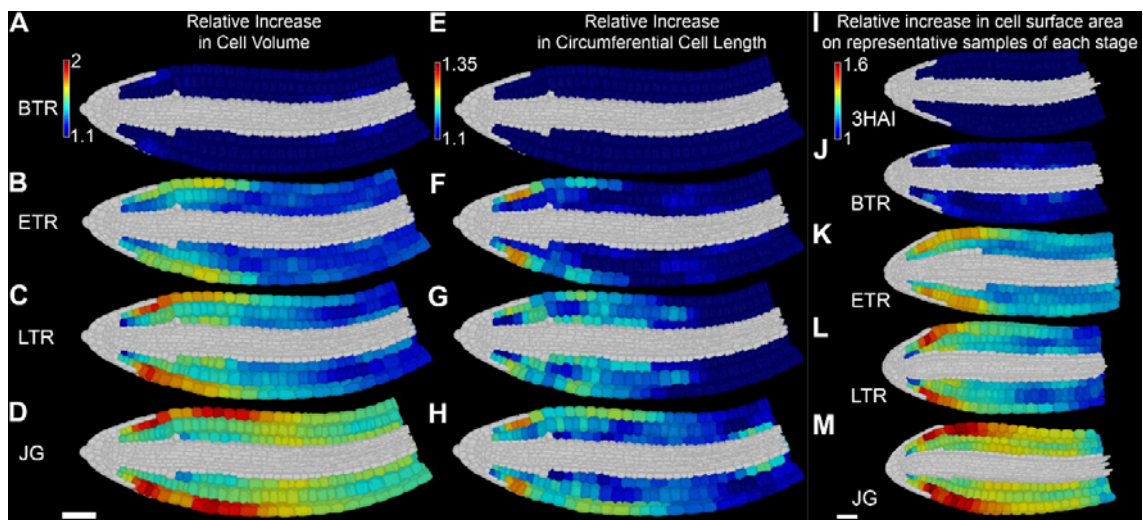
2

3 **ATHB5 regulates GA-mediated plasticity in hypocotyl cell growth during Arabidopsis seed**
4 **germination**

5

6 *Petra Stamm, Alexander T. Topham, Nur Karimah Mukhtar, Matthew D. B. Jackson, Daniel*7 *F. A. Tomé, Jim L. Beynon, George W. Bassel*

8

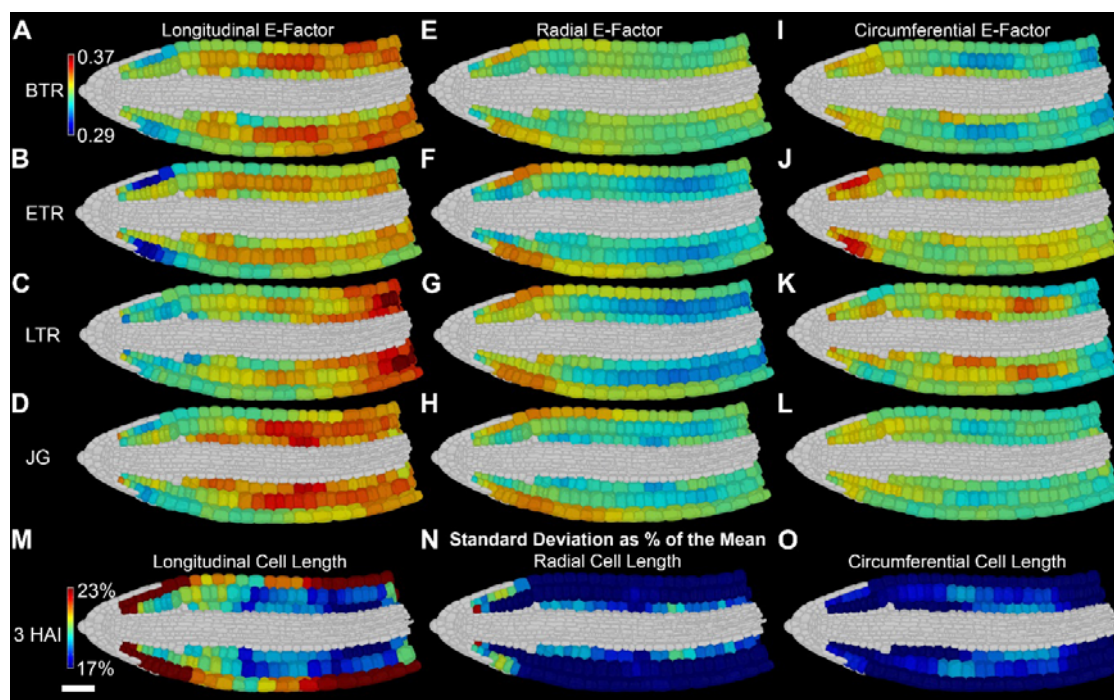


9

10 **Supplemental Fig. 1, Related to Fig. 1.** Quantification of changes in 3D cell shape of the
11 *Arabidopsis* embryo during germination at single cell resolution.12 Mean relative increase in cell volume (A-D) and circumferential cell length (E-H) compared
13 to unexpanded embryos (3 HAI) over the course of germination, at (A, E) BTR, (B, F) ETR,
14 (C, G) LTR and (D, H) JG. Data were derived from four embryos. Mean size and length of
15 each individual cell was calculated, and the ratio over the corresponding mean of
16 unexpanded embryos (3 HAI) was determined. Scale bar for (A-H) in (D) is 50 μm . (I-M)
17 Mean relative increase in cell surface area, as in Fig. 1, false-coloured onto cellular meshes
18 representative of each stage, (I) at the unexpanded state (3 HAI), at (J) BTR, (K) ETR, (L)
19 LTR and (M) JG. Scale bar for (I-M) in (M) is 50 μm .

20

21

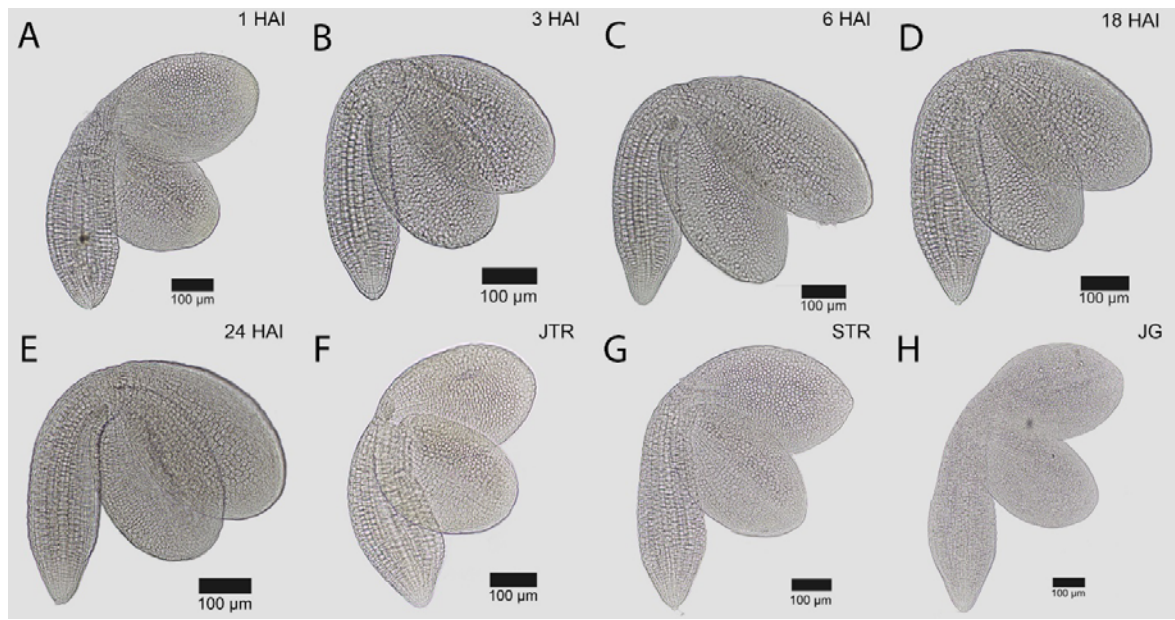


22

23 **Supplemental Fig. 2, Related to Fig. 1.** 3D Anisotropy of cell shape change driving
 24 *Arabidopsis* germination, and variability of cell lengths.

25 E-Factors describe the relative contribution of cell anisotropy in a given direction divided by
 26 the total anisotropy in all 3 principal directions. (A-D) Longitudinal, (E-H) radial, and (I-L)
 27 circumferential E-Factors at (A, E, I) BTR, (B, F, J) ETR, (C, G, K) LTR and (D, H, L) JG
 28 during germination. False colouring for E-factors is the same for all axes ranging from 0.29
 29 to 0.37. Higher values in the red scale indicate a greater contribution to overall growth, while
 30 lower values in the blue scale indicate less contribution relative to the overall 3D anisotropy
 31 of an individual cell. (M-O) Cellular embryo meshes false-coloured to show the standard
 32 deviation of different cell lengths in unexpanded embryos (3 HAI). Individual cell lengths of
 33 unexpanded embryos were pooled according to cell type and position, and the standard
 34 deviation of each metric was determined as a percentage of the mean. Standard deviation
 35 for (M) longitudinal, (N) radial and (O) circumferential cell lengths are shown. Scale bar for
 36 all in (M) is 50 μm .

37

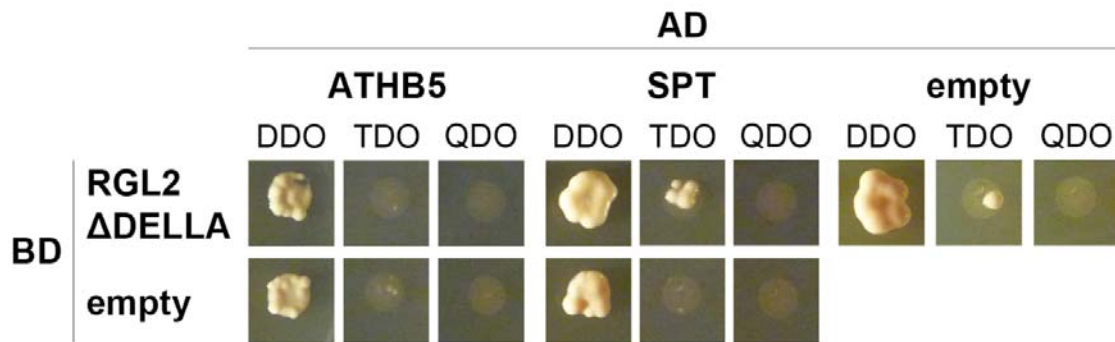


38

39 **Supplemental Fig. 3. Distribution of the RGL2 protein during non-dormant seed**
40 **germination.** A reporter construct *RGL2::RGL2-GUS* consisting of 2 kb upstream sequence
41 of the RGL2 gene and a C-terminal in frame GUS fusion was imaged using light microscopy
42 of germinating non-dormant *Arabidopsis* seeds. No signal was detected after 4 days of GUS
43 staining at 37 °C in 8 independent lines.

44

45



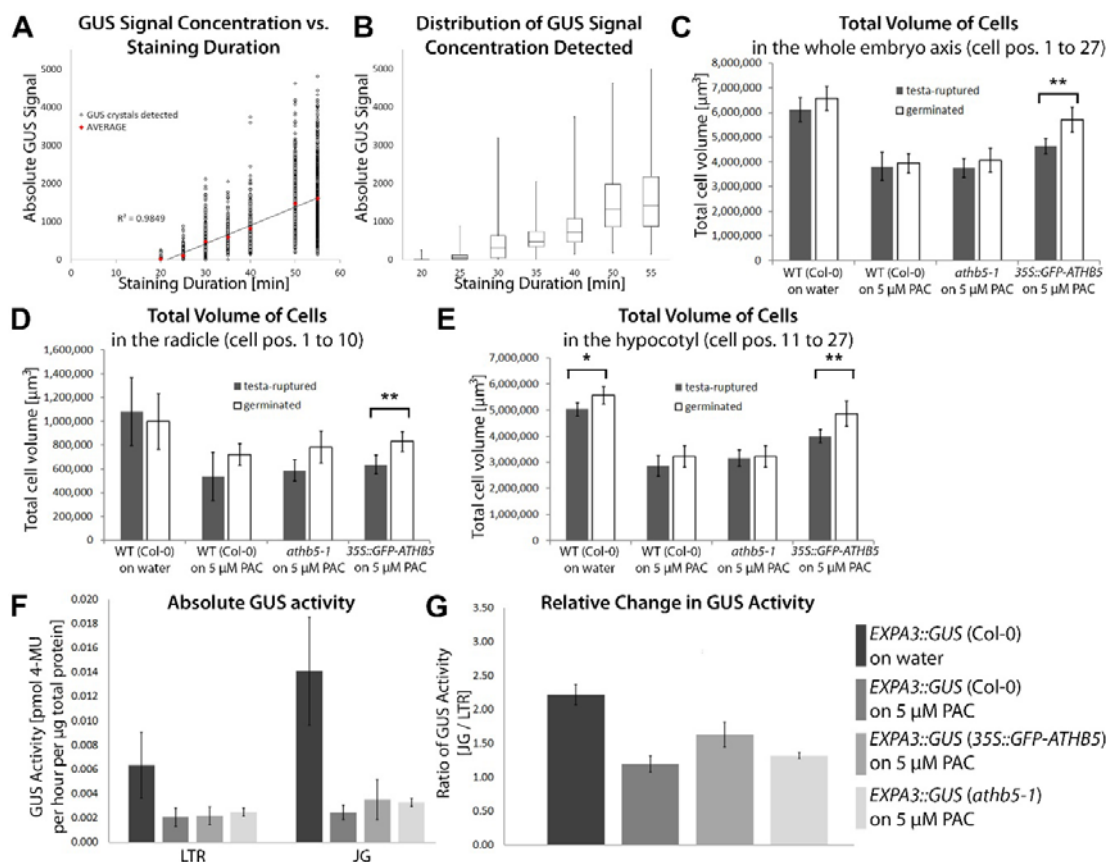
46

47 **Supplemental Fig. 4, Related to Figs. 2 and 3.** A yeast two-hybrid assay was performed to
 48 test for interaction of ATHB5 with RGL2. A truncated version of RGL2, lacking the DELLA
 49 domain (conferring self-activation in yeast) was used as bait. Interactions were tested with
 50 ATHB5, and SPATULA (SPT) as positive control. Plating onto SD medium lacking Trp and
 51 Leu (double drop-out medium, DDO) served as a positive growth control. Strength of
 52 interactions were determined on SD medium lacking Trp, Leu, His (triple drop-out, TDO) and
 53 SD medium lacking Trp, Leu, His and Ade (quadruple drop-out, QDO).

54

55

56



57

58 **Supplemental Fig. 5, Related to Figs. 4 and 5.**

59 (A-B) Relationship between GUS staining duration and GUS quantity measured in
 60 MorphoGraphX. GUS reporter concentration within individual epidermal cells was
 61 determined using MorphoGraphX in 35S::GUS *Arabidopsis* embryos stained for increasing
 62 periods of time. (A) Plot of absolute GUS concentration within individual epidermal cells of
 63 four embryos stained for increasing periods of time, as detected by confocal imaging, without
 64 normalization. Average GUS quantities for each time point are indicated by red diamonds.
 65 The trend line and regression coefficient are included within the plot. This represents an
 66 equivalent analysis to pooling data at single cell resolution and statistically analysing mean
 67 GUS reporter abundance. (B) Box and whisker plot to show the distribution of GUS activities
 68 detected in individual epidermal cells of four embryos. Central line is the median, box ends
 69 are the 25th and 75th percentiles, and whiskers cover the range of data. (C-E) Quantification
 70 of total cell volumes during embryo growth. The sum of cell volumes of all cell types was
 71 determined for the whole embryo axis (cell positions 1 to 27), and separately for the radicle
 72 (cell positions 1 to 10) and the hypocotyl (cell positions 11 to 27). (C) Total cell volumes of
 73 the whole embryo axis in embryos of testa-ruptured (grey bars) and germinated (white bars)
 74 seeds on water and on 5 μM PAC. (D) Total cell volumes of the radicle in embryos of testa-
 75 ruptured (grey bars) and germinated (white bars) seeds on water and on 5 μM PAC. (E)

76 Total cell volumes of the hypocotyl in embryos of testa-ruptured (grey bars) and germinated
77 (white bars) seeds on water and on 5 μ M PAC. Asterisks indicate significant differences, as
78 determined by a Student's t-test, with $p < 0.05$ (one asterisk) and $p < 0.01$ (two asterisks),
79 respectively. (F-G) Quantification of GUS activity in embryos during imbibition on PAC. (F)
80 GUS activity in dissected embryos of *EXPA3::GUS* in WT, *35S::GFP-ATHB5* and *athb5-1*
81 background imbibed on 5 μ M PAC. GUS activity of water-imbibed *EXPA3::GUS* embryos
82 was included for comparison (see Supplemental File S2). LTR represents step 1 and testa
83 rupture, and JG the completion of step 2. (G) Relative change in GUS activity at JG,
84 compared to LTR, for each sample shown in (F).

85

86 **Supplemental Table**

87 **Supplemental Table 1, Related to Figs. 1, 4 and 5.** Linear regression examining
 88 relationships between ATHB5 protein abundance, *EXPA3* promoter activity and changes
 89 in cell surface area across different cell types of the *Arabidopsis* embryonic hypocotyl (cell
 90 positions 11 to 35).
 91

Stage	Cell Type	ATHB5 and Cell Growth		<i>EXPA3</i> and Cell Growth		ATHB5 and <i>EXPA3</i>	
		R ²	p-value	R ²	p-value	R ²	p-value
ETR	Epidermis	0.101	1.72•10 ⁻⁰¹	0.24	3	0.60	4.91•10 ⁻⁰⁵
	Outer Cortex	0.249	2.52•10 ⁻⁰²	0.16	4	0.91	7.70•10 ⁻¹¹
	Inner Cortex	0.152	8.95•10 ⁻⁰²	0.15	0	0.94	1.41•10 ⁻¹²
	Water	0.628	3.12•10 ⁻⁰⁵	0.67	5	0.86	4.10•10 ⁻⁰⁹
LTR	Outer Cortex	0.755	6.79•10 ⁻⁰⁷	0.80	4	0.90	1.11•10 ⁻¹⁰
	Inner Cortex	0.191	5.43•10 ⁻⁰²	0.16	8	0.80	7.22•10 ⁻⁰⁸
	Water	0.805	8.34•10 ⁻⁰⁸	0.60	8	0.83	2.13•10 ⁻⁰⁸
	Outer Cortex	0.707	3.42•10 ⁻⁰⁶	0.73	3	0.94	7.47•10 ⁻¹³
JG	Inner Cortex	0.392	3.14•10 ⁻⁰³	0.30	0	0.80	9.91•10 ⁻⁰⁸
	Outer Cortex	0.392	3.14•10 ⁻⁰³	0.30	0	1.25•10 ⁻⁰²	1

R² indicates the fraction of the variation in the dependent variable (increase in cell surface area and *EXPA3* promoter activity, respectively) accounted for by the independent variable (ATHB5 protein abundance and *EXPA3* promoter activity, respectively). A P value < 0.05 represents a significant relationship.

92

93

94 **Supplemental Items**

95 **Supplemental File 1, Related to Fig. 1.** Cellular growth data.

96 Excel workbook containing all raw data and graphs related to growth. Each tab contains the
97 mean relative increase in cell volume, cell surface area, as well as longitudinal, radial and
98 circumferential cell lengths for each cell type and each cell position along the embryo axis for
99 a particular stage, compared to the unexpanded embryos (3 HAI). Each metric is given with
100 its corresponding 95% confidence interval (green dashed line) based on the t-distribution.

101

102 **Supplemental File 2, Related to Fig. 5.** Cellular GUS reporter abundance data.

103 Excel workbook containing all raw data and graphs relating to reporter quantification. Each
104 tab contains the mean concentration of GUS abundance in individual cells measured by
105 confocal microscopy, normalised using the quantified GUS activity using fluorometric
106 assays. Each cell type and each cell position along the embryo axis for a particular stage is
107 provided. Each metric is given with its corresponding 95% confidence interval.

108

109 **Supplemental Movie 1, Related to Fig. 1.** Dynamics of cell growth across *Arabidopsis*
110 seed germination.

111 False-coloured cellular organ meshes of embryonic axes displaying (clockwise from top left)
112 changes in cell surface area, cell volume, longitudinal cell length and radial cell lengths in
113 embryos during seed germination. Heat values between measured time points have been
114 extrapolated to represent transitions between samples stages.

115

116 **Supplemental Movie 2, Related to Fig. 5.** Dynamics of cell growth, *EXPA3* promoter
117 activity and *ATHB5* protein abundance across *Arabidopsis* seed germination.

118 False-coloured cellular organ meshes of embryonic axes displaying (clockwise from top left)
119 changes in cell surface area, longitudinal cell length, *EXPA3* promoter activity and *ATHB5*
120 protein abundance throughout steps 1 and 2 of seed germination. Heat values between
121 measured time points have been extrapolated to represent transitions between sampled
122 stages.

123

124 **Literature Cited**

125 **Johannesson H, Wang Y, Engstrom P** (2001) DNA-binding and dimerization preferences
126 of *Arabidopsis* homeodomain-leucine zipper transcription factors in vitro. *Plant Molecular*
127 *Biology* **45**: 63-73

128